Supplementary Material of "Temporal interpretability of latent dynamics in supervision-free bioinformatics"

Wenjun Bai, Okito Yamashita, and Junichiro Yoshimoto Department of Computational Brain Imaging
Neural Information Analysis Laboratories
Advanced Telecommunication Research International (ATR)
Kyoto, Japan
Email: {wjbai, oyamashi, jun-y}@atr.jp

I. Training configurations in the proof-of-concept study

We applied seven instantiations of our mutual information-based predictive framework to the simulated high-dimensional dynamics, i.e., $[T = 2000, L = 100]$ for learning seven types of latent dynamics. Importantly, we split the entire dataset into halves, 1st half to serve the training data, whereas the 2nd half to serve for the test data. Thus, each type of learned latent dynamics attains the size of $[T = 1000, l = 100]$.

Each training configuration for seven models is unfolded as follows.

1) $I(x, \mathcal{E}_\phi(z))$ As maximising this term is equivalent with training an auto-encoder model to reproduce the original dynamics, thus, we trained a simple **five** layer neural network, i.e., number of nodes in five layers are:$[100 \rightarrow 20 \rightarrow 3 \rightarrow 20 \rightarrow 100]$, with the ReLU nonlinearity to learn ϕ.
2) $I(xx^\top, zz^\top)$ Similar with the previous implementation, here, we harness a simple **three** layer neural network without the decoder, i.e., number of nodes in three layers are:$[100 \rightarrow 20 \rightarrow 3]$. We then compute the $xx^\top$ and $zz^\top$ by using the innate `tf.transpose` function in the `tensorflow` library.
3) $\mathcal{L}_{1st}$ We merge the first two implementations together with a five layer neural network, i.e., number of nodes in five layers are:$[100 \rightarrow 20 \rightarrow 3 \rightarrow 20 \rightarrow 100]$ here.
4) $I(z_t, z_{t'})$ We utilized the Gate Recurrent Unit (GRU) to serve as a nonlinear autoregressive function $f_{z_t}(z_t, z_{t'})$, the rest configuration is identical to the $I(x, \mathcal{E}_\phi(z))$ instantiation.
5) $I(J_{z_t}, J_{z_{t'}})$ We adopted a similar implementation with the $I(z_t, z_{t'})$ instantiation with one extra layer to compute the Jacobain for each subsequence. We then aggregate the Jacobians over all subsequences to form a huge Jacobian matrix of the entire to-be-learned dynamics for QR decomposition. The diagonal part of the resultant matrix after QR decomposition was served as our loss term to optimize the entire neural network.
6) $\mathcal{L}_{2nd}$ We optimized the network through minimizing both loss terms from the GRU in $I(z_t, z_{t'})$ and previous term in $I(J_{z_t}, J_{z_{t'}})$ simultaneously.
7) $\mathcal{L}_{1st}$ & $\mathcal{L}_{2nd}$ We aggregated all the loss terms together with the inserted `tf.sigmoid` function to adjust each loss terms to be $[0, 1]$.

Additionally, the configurations of three alternative embedding approaches: PCA, MDS, and t-SNE were disclosed here. We adopted the default settings of PCA and MDS in `sklearn` library to yield their respective latent dynamics. For t-SNE, we set the perplexity to 30, number of iteration to 500 to produce the t-SNE latent dynamics.

II. Supplementary results on Motion data

Similar to the implementation of $\mathcal{L}_{1st}$ & $\mathcal{L}_{2nd}$ in the proof-of-concept study, to learn behavior - and subject-wise latent dynamics from the high-dimensional biometric (motion) data, we trained the $\mathcal{L}_{1st}$ & $\mathcal{L}_{2nd}$ model with first half of data, then applied to the second half, and vice versa. Thereby, we are able to mine latent dynamics for all behavior conditions (4 conditions) and subjects (4 subjects).

In addition to the results in the main text that are yielded from averaging over the sessions, here, we also showcase the session-wise latent dynamics for standing, walking, running, and badminton behavior conditions, respectively.

From the presented session-wise latent dynamics, it is evident that the these dynamics are consistent across sessions for all behavior types.

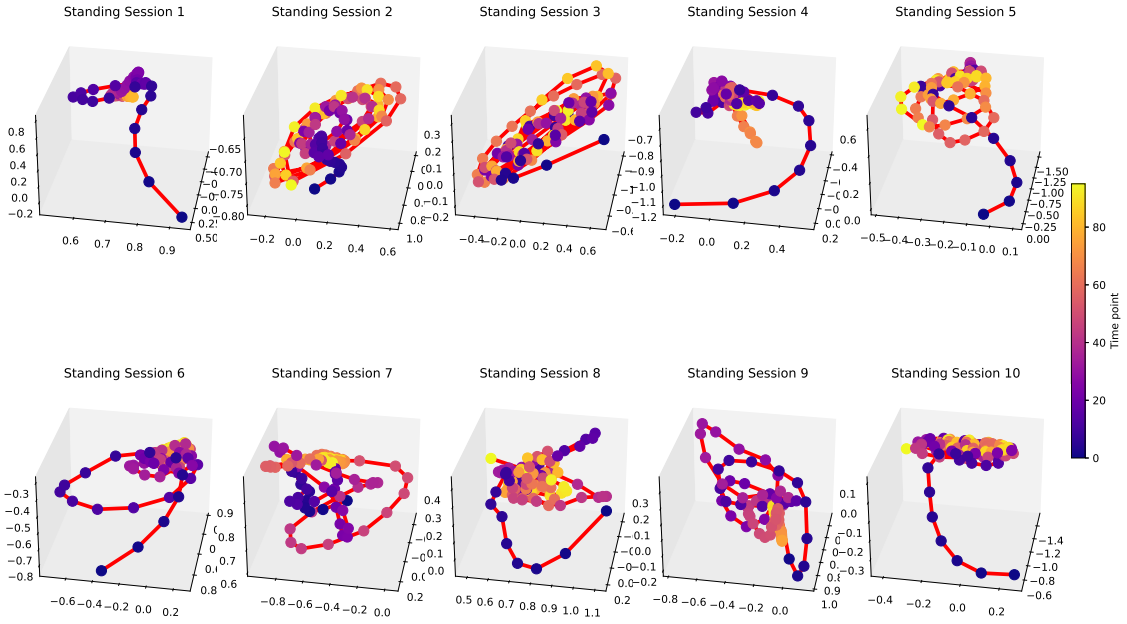

Fig. 1: Session-wise latent dynamics for the standing condition

REFERENCES

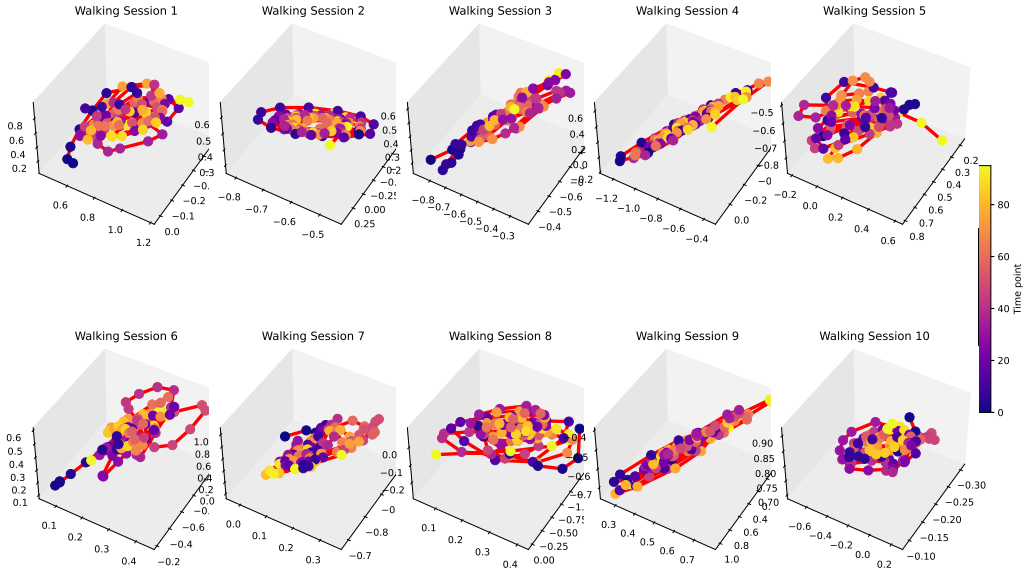

Fig. 2: Session-wise latent dynamics for the walking condition

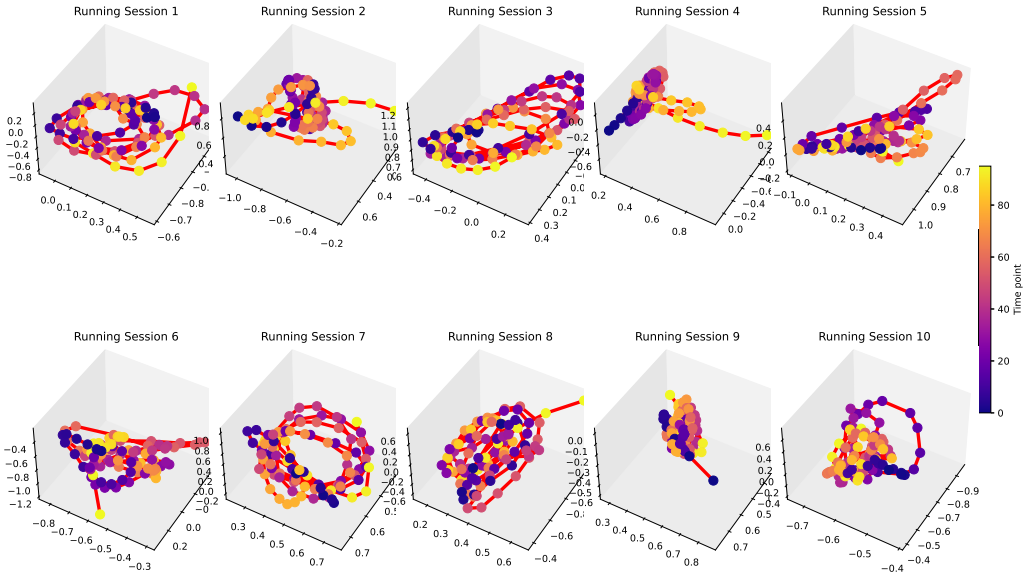

Fig. 3: Session-wise latent dynamics for the running condition

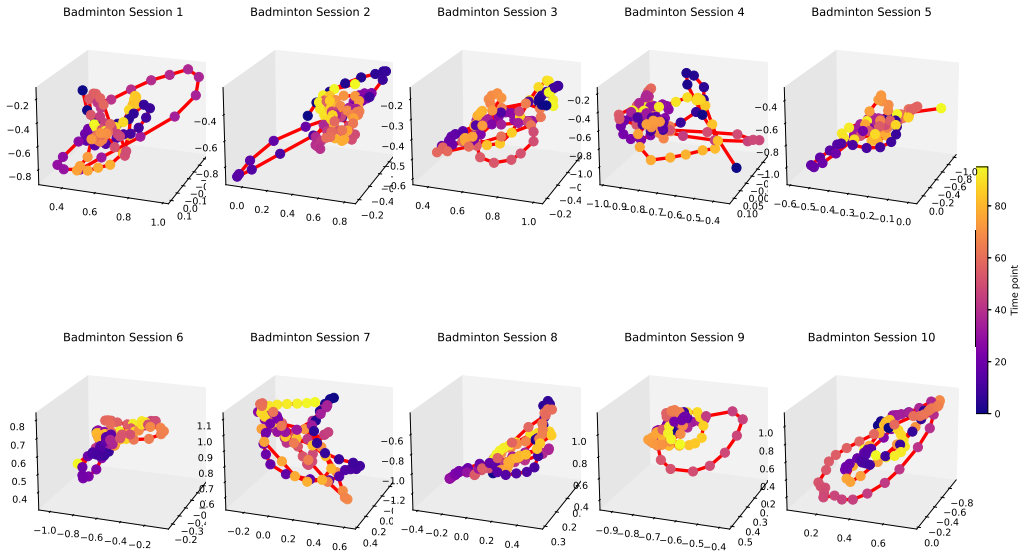

Fig. 4: Session-wise latent dynamics for the badminton condition